CONTINUUM VERSUS STRUCTURAL APPROACH TO STABILITY OF REINFORCED SOIL

By Radoslaw L. Michalowski,[1] Member, ASCE, and Aigen Zhao,[2] Student Member, ASCE

ABSTRACT: Two techniques for stability analysis of reinforced soil structures are presented. In the first one, called the continuum approach here, the reinforced soil is first homogenized, and the slip-line method is used to find the limit stress field in an anisotropic continuum. The second, structural approach, considers reinforcement and granular fill as two separate structural components, and the kinematical method of limit analysis is used as the technique of solution. The solutions to critical heights of reinforced slopes are presented as an illustrative example for application of the described techniques. The structural approach proposed here has a clear theoretical interpretation, is easily applicable to any failure patterns, and can be modified to accommodate the nonassociative flow rule for soils. The continuum approach with the slip-line method of solution for stresses was found to be more restrictive and less convenient than the structural approach. The continuum approach is expected to have a wider application, however, in analysis of earth structures with less conventional reinforcements such as continuous filament or for fiber-reinforced soils.

INTRODUCTION

The existing methods for design of reinforced soil structures have two very clear areas of consideration: the mechanics part, and the portion relating to technology of construction, durability, and so on. In recent years more emphasis has been placed on introducing "partial" factors and additional coefficients rather than improving the mechanics considerations. The present paper is devoted to the mechanics of failure of reinforced soil, and it demonstrates how the reinforcement can be included in analyses more rigorous than those in practice today.

Stability of reinforced soil structures is most often analyzed by using the traditional methods based on the limit equilibrium approach. Such analyses can be found, for example, in papers by Leshchinsky and Volk (1985), Schmertmann et al. (1987), Jewell (1990), and others. Different avenues are explored in the present paper. Rather than including the reinforcement forces in the global equilibrium equations for collapsing blocks, the local equations of equilibrium for an "equivalent continuum" are used. This technique is called a "continuum approach" here. A similar approach to stability analysis has been suggested in the last few years (de Buhan et al. 1989; Sawicki and Leśniewska 1989), and it is proposed that its feasibility as a design technique be assessed critically in view of other methods. The second technique proposed uses the kinematic approach of limit analysis and is called a "structural approach" here, since both the reinforcement and the granular fill are considered two separate structural components. Application of limit analysis theorems in stability considerations of reinforced soil was earlier indicated by Anthoine (1989) and Michalowski (1992).

In the continuum approach, the reinforced soil mass is homogenized first, and the local (differential) equations of equilibrium are used so that a balanced stress state is found throughout the failing soil mass. The idea of homogenization and describing the strength of the reinforced soil in terms of the limit macroscopic stress state for an "equivalent continuum" originates from analyses of composite materials. It was applied to reinforced soils in the 1970s (Romstad et al. 1976) to represent the stress-strain relation of reinforced soil, and, more recently, it was used to represent the yield criterion of reinforced soils (Sawicki 1983; de Buhan et al. 1989).

The formulation of the macroscopic failure criterion for reinforced soil found in Sawicki (1983) and de Buhan et al. (1989) is derived from a purely static approach based on summation of stresses in the constituents of the reinforced soil. An alternative formulation, based on the kinematical approach to homogenization of soils, was used by Michalowski and Zhao (1993). The kinematical approach to homogenization was suggested earlier for a plane stress problem (filament-reinforced membrane) by McLaughlin and Batterman (1970). While both the static and kinematic approach are conceptually equally simple and lead to identical macroscopic yield functions for the simple case of unidirectionally reinforced soil, there are some advantages in

[1]Assoc. Prof., Dept. of Civ. Engrg., Johns Hopkins Univ., Baltimore, MD 21218.
[2]Des. Engr., Tenax Corp., formerly Grad. Student, Dept. of Civ. Engrg., Johns Hopkins Univ., Baltimore, MD.

Note. Discussion open until July 1, 1995. To extend the closing date one month, a written request must be filed with the ASCE Manager of Journals. The manuscript for this paper was submitted for review and possible publication on August 3, 1993. This paper is part of the ***Journal of Geotechnical Engineering***, Vol. 121, No. 2, February, 1995. ©ASCE, ISSN 0733-9410/95/0002-0152–0162/$2.00 + $.25 per page. Paper No. 6643.

using the kinematic approach when considering both tensile failure and slip in fiber-reinforced soils (Michalowski and Zhao 1994). Here, only the traditional (unidirectional) reinforcement is considered, and only the static approach is used. It should be mentioned that there is a considerable body of French literature from the 1980s in the area of homogenization as applied to reinforced soil. Some references are cited in de Buhan and Taliercio (1991).

Differential equations describing the limit state for an equivalent anisotropic continuum are of a hyperbolic type and can be solved using the method of characteristics (slip-line method). Such approach has been very widely applied in stability analyses of isotropic soils (Sokolovskii 1965), but few applications to anisotropic pressure-sensitive soils can be found (Booker and Davis 1972). The slip-line method was applied by Sawicki and Leśniewska (1989) to find limit loads on reinforced soil slopes. The approach in the present paper is also based on solving the stress equations using the method of characteristics, but it differs from that proposed by Sawicki and Leśniewska (1989) in the formulation of the failure condition and in the form of the slip-line equations. The relations here do not contain the Heaviside function for "switching on" the reinforcement.

The objective of the present paper is to research the feasibility of the continuum approach in stability analyses of earth structures with reinforcing bars or grids, and to examine whether any advantages over a more conventional structural approach exist. The continuum approach is applicable to densely reinforced structures, that is, structures with repeated layers of reinforcement with spacing that is small with respect to the dimensions of the entire structure.

Furnishing an exact ratio of the reinforcement spacing to the structure size, below which the structure can be homogenized in the analysis, must carry some engineering intuition. Such criterion can be approximately determined through comparison of analyses where identical structures are considered using both the continuum and the structural approaches. The applicability of the continuum approach does not require that the reinforced soil behave like a microscopically homogeneous system. It is only necessary to indicate that the predictions for which the method is intended (limit loads on structures, critical heights) are reasonably close to those from a less presumptive structural approach. Preliminary calculations indicate that the continuum approach may be less restrictive than intuitively conjectured. For instance, a critical height of about 12 m for a wall (with surcharge load) reinforced with eight evenly-spaced layers of specified reinforcement (granular backfill) was predicted by both techniques with a difference of less than 5%. Specific guidelines as to when the reinforced soil can be considered a uniform continuum will probably be structure-dependent, and are yet to be studied. It is more appropriate to investigate them when developing design procedures for specific structures.

The failure criterion for a homogenized reinforced soil is presented in the next section, followed by the slip-line solution to the problem of a reinforced slope. Application of the structural approach is also shown, and the two approaches are discussed in the final section.

HOMOGENIZATION AND MACROSCOPIC FAILURE CRITERION

Calculations of the macroscopic stress in a densely reinforced soil are based here on the summation of the stresses in the respective constituents, as in mixtures. Accordingly, the macroscopic stress state in the reinforced composite ($\bar{\sigma}_{ij}$) is represented as

$$\bar{\boldsymbol{\sigma}}_{ij} = \eta^m \boldsymbol{\sigma}^m_{ij} + \eta^r \boldsymbol{\sigma}^r_{ij} \qquad i, j = 1, 2, 3 \tag{1}$$

where $\boldsymbol{\sigma}^r_{ij}$ and $\boldsymbol{\sigma}^m_{ij}$ = stress tensors in the reinforcement and in the matrix material, respectively; and η^r and η^m = the respective volume fractions. If the volume of the reinforcement is considered negligible with respect to the matrix volume, $\eta^m >> \eta^r$, then for a unidirectionally reinforced composite the macroscopic stress tensor becomes

$$\bar{\boldsymbol{\sigma}}_{ij} = \bar{\boldsymbol{\sigma}}^m_{ij} + \xi k_t \boldsymbol{n}_i \boldsymbol{n}_j; \qquad i, j = 1, 2, 3 \tag{2}$$

where k_t = tensile strength of reinforcement per unit cross section of the entire composite; ξ = a coefficient indicating the mobilization of the reinforcement strength; and $\boldsymbol{n}_i$ = unit vector in the direction of the reinforcement. The ability of the reinforcement to withstand compression is neglected here (owing to buckling and kinking) and the range of variability of ξ is restricted to $-1 \leq \xi \leq 0$ (compression taken as positive). The influence of the confining pressure on the tensile collapse load of the reinforcement is neglected here. For a uniformly placed reinforcement, k_t can be calculated as

$$k_t = \frac{T}{d} \tag{3}$$

where T = limit force per unit length of reinforcement (when the reinforcement is in the form of sheets of geotextile or geogrid); and d = vertical spacing. For reinforcing bars or strips, k_t can be taken as $T/d_1 d_2$ (T = tensile limit force of a single bar or strip; d_1, d_2 = horizontal and vertical spacing).

The homogenization technique is used to derive the yield criterion for the reinforced composite under plane strain conditions. Yielding of a reinforced soil composite occurs due to yielding of both the soil matrix and the reinforcement, or it may occur due to yielding of the matrix alone. As the failure condition for the homogenized reinforced soil is anisotropic, it is convenient to represent the stress state in terms of parameters p, q, and ψ defined as

$$p = \frac{\bar{\sigma}_x + \bar{\sigma}_y}{2}; \qquad q = \frac{\bar{\sigma}_x - \bar{\sigma}_y}{2}; \qquad \tan 2\psi = \frac{2\bar{\tau}_{xy}}{\bar{\sigma}_x - \bar{\sigma}_y} \tag{4}$$

and to illustrate the yield surface in space p, q, and $\bar{\tau}_{xy}$ (Figs. 1 and 2). In (4), $\bar{\sigma}_x$, $\bar{\sigma}_y$, and $\bar{\tau}_{xy}$ are the macrostresses in the composite. As in the case of the standard Mohr-Coulomb yield condition, the yield function for homogenized reinforced soil is independent of the intermediate principal stress. The reinforcement, if in the form of bars, is considered to be in the x, y-plane.

Fig. 1 presents a cross-section of the p, q, $\bar{\tau}_{xy}$-space with plane p = constant. Each of the circles was obtained from (2) assuming a different mobilization of the tensile strength in the reinforcement, and the stress state in the matrix material satisfied the Mohr-Coulomb yield condition

$$(\sigma_x^m + \sigma_y^m)\sin\varphi - \sqrt{(\sigma_x^m - \sigma_y^m)^2 + 4\tau_{xy}^2} = 0 \tag{5}$$

where φ = the internal friction angle. The reinforcement is inclined to the x-axis at angle α and the components of the unit vector $\mathbf{n}_i$ and $\mathbf{n}_j$ in (2) are $n_x = \cos\alpha$, $n_y = \sin\alpha$, and $n_z = 0$. The matrix material here is considered to have no cohesion. The circle for $\xi = 0$ represents failure states typical of isotropic materials and the circle for $\xi = -1$ shows yielding of the composite with a fully stressed reinforcement (in tension). The envelope of all the circles constitutes the macroscopic failure criterion for the composite. The straight-line segments of this criterion represent failure of the composite with intermediate mobilization of the force in the reinforcement: $-1 < \xi < 0$. The surface in space p, q, $\bar{\tau}_{xy}$, see Fig. 2, represents the macroscopic failure criterion, and it consists of two conical segments and two plane sections. A similar criterion (in a different stress space) was shown by de Buhan and Siad (1989). It can be argued that if the yielding macrostress state for a composite element is interpreted as the limit load on an "elementary structure," then the static approach used here leads to a "safe" estimate of these loads.

Representation of failure surface $f(p, q, \bar{\tau}_{xy}) = 0$ can be described as a piecewise function. For convenience, radius R (stress invariant) is introduced as shown in Fig. 1.

$$R = \sqrt{q^2 + \bar{\tau}_{xy}^2} = \frac{1}{2}\sqrt{(\bar{\sigma}_x - \bar{\sigma}_y)^2 + 4\bar{\tau}_{xy}^2} \tag{6}$$

For the part where no influence of reinforcement is present ($\xi = 0$), the analytic representation of the macroscopic yield function is

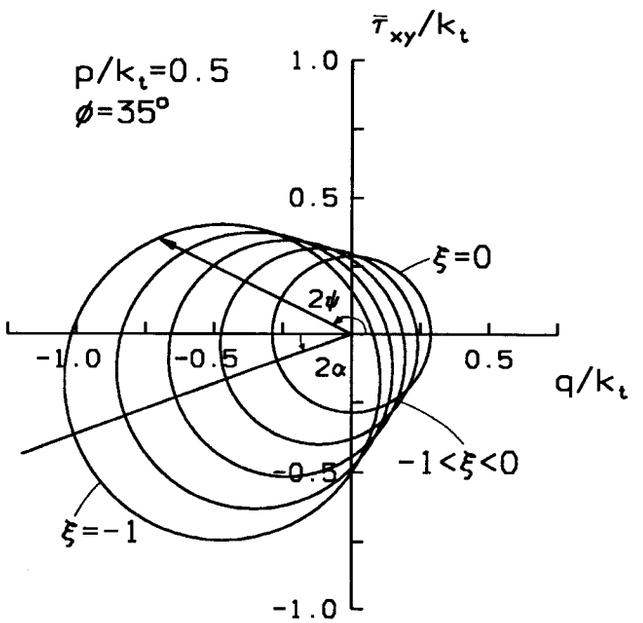

FIG. 1. Limit Stress States with Different Mobilization of Reinforcement Strength (Space p, q, $\bar{\tau}_{xy}$)

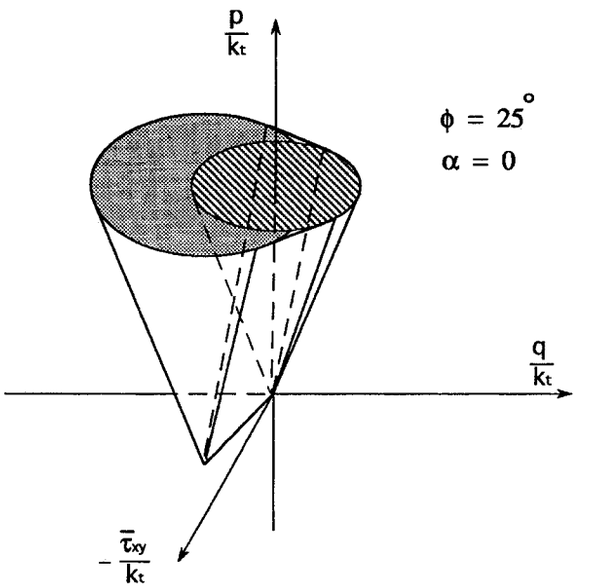

FIG. 2. Macroscopic Yield Condition in p, q, $\bar{\tau}_{xy}$-Space for Unidirectionally Reinforced Soil

$$\frac{R}{k_t} = \frac{p}{k_t} \sin\varphi; \quad |2\psi - 2\alpha| \le \frac{\pi}{2} - \varphi \tag{7}$$

where α = angle of inclination of the reinforcement to the x-axis; for planar segments ($-1 < \xi < 0$)

$$\frac{R}{k_t} = \frac{p}{k_t} \frac{\sin\varphi}{\sin(2\psi + \varphi - 2\alpha)}; \quad \frac{\pi}{2} - \varphi < |2\psi - 2\alpha| \le \frac{\pi}{2} - \varphi + \tan^{-1}\left(\frac{k_t}{2p \tan\varphi}\right) \tag{8}$$

and when the strength in the reinforcement is fully mobilized ($\xi = -1$)

$$\frac{R}{k_t} = -0.5\cos(2\psi - 2\alpha) + \sqrt{\left(\frac{p}{k_t} + 0.5\right)^2 \sin^2\varphi - 0.25\sin^2(2\psi - 2\alpha)};$$

$$\frac{\pi}{2} - \varphi + \tan^{-1}\left(\frac{k_t}{2p \tan\varphi}\right) < |2\psi - 2\alpha| \le \pi \tag{9}$$

SLIP-LINE SOLUTION IN CONTINUUM APPROACH

The macroscopic yield condition for the reinforced soil under plane strain conditions can be represented as

$$f(\bar{\sigma}_x, \bar{\sigma}_y, \bar{\tau}_{xy}) = R - F(p, \psi) = 0 \tag{10}$$

where R, p, and ψ are given in (4) and (6). When function F is independent of ψ, (10) represents an isotropic yield criterion. Specific functions $F(p, \psi)$ for different segments of the macroscopic failure criterion for the reinforced soil are given in (7)–(9). Eq. (10) along with the set of differential equilibrium equations

$$\frac{\partial\bar{\sigma}_x}{\partial x} + \frac{\partial\bar{\tau}_{xy}}{\partial y} = 0; \qquad \frac{\partial\bar{\tau}_{yx}}{\partial x} + \frac{\partial\bar{\sigma}_y}{\partial y} = -\gamma \tag{11a,b}$$

leads to a set of two hyperbolic-type partial differential equations that can be solved using the method of characteristics. Following Booker and Davis (1972), the equations of characteristics can be expressed as

$$\frac{dy}{dx} = \tan(\psi - m - \nu); \qquad \text{along } s_1 - \text{characteristic} \tag{12a}$$

$$\frac{dy}{dx} = \tan(\psi - m + \nu); \qquad \text{along } s_2 - \text{characteristic} \tag{12b}$$

and the stress relations along the characteristics are

$$\sin[2(m - \nu)]\frac{\partial p}{\partial s_1} + 2F\frac{\partial\psi}{\partial s_1} + \gamma\cos(2m)\left[\cos(2\nu)\frac{\partial x}{\partial s_1} - \sin(2\nu)\frac{\partial y}{\partial s_1}\right] = 0; \qquad s_1 \tag{13a}$$

$$\sin[2(m + \nu)]\frac{\partial p}{\partial s_2} + 2F\frac{\partial\psi}{\partial s_2} + \gamma\cos(2m)\left[\cos(2\nu)\frac{\partial x}{\partial s_2} + \sin(2\nu)\frac{\partial y}{\partial s_2}\right] = 0; \qquad s_2 \tag{13b}$$

and

$$\tan(2m) = \frac{1}{2F}\frac{\partial F}{\partial\psi}; \qquad \cos(2\nu) = \cos(2m)\frac{\partial F}{\partial p} \tag{14}$$

where γ = unit weight of the soil. The gravity acceleration is assumed here to be directed opposite to coordinate y. These equations are considerably different from those of Sokolovskii (1965) for isotropic materials.

The slip-line fields shown in Fig. 3 are for two slopes whose internal friction angles of the matrix material are 30° and 40°, respectively. The boundary condition along AO [Fig. 3(a)] must be given in terms of p and ψ. In the absence of traction on AO, $\psi = \beta$ (β-slope inclination angle). Parameter p at AO is calculated from equilibrium equations for a composite element adjacent to AO, assuming yielding of the composite with a fully mobilized tensile strength in the reinforcement ($\xi = -1$)

$$p = \frac{k_t}{2\cos^2\varphi}\left[(\sin^2\varphi - \cos 2\beta) + \sqrt{(\cos 2\beta + \cos 2\varphi)(\cos 2\beta - 1)}\right] \tag{15}$$

The solution to p on AO can be obtained from (15) when $\beta \ge \pi/2 - \varphi$. Condition $\beta < \pi/2 - \varphi$ is indicative of less than full mobilization of strength in the reinforcement.

Having determined the stress boundary condition at AO, the Cauchy boundary value problem

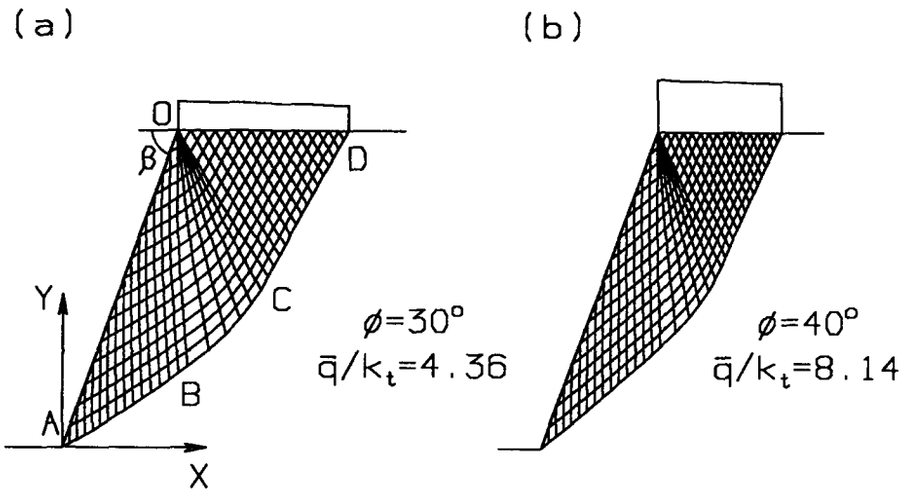

FIG. 3. Slip-Line Fields for Two 70° Reinforced Slopes ($\gamma H/k_t$ = 0.76): (a) φ = 30°; and (b) φ = 40°

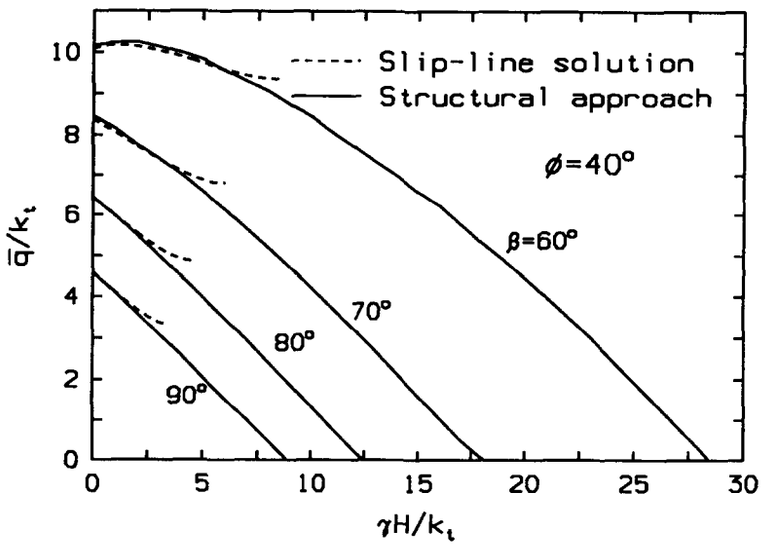

FIG. 4. Average Limit Pressure on Slopes as Function of Slope Characteristic Number $\gamma H/k_t$; Comparison of Two Methods

was solved first in region AOB [Fig. 3(a)], followed by the characteristic problem in area OBC with a singular point at O, and then the problem with mixed boundary conditions in COD (traction assumed vertical at OD). Once p along OD was found ($\psi = \pi/2$), tractions were computed. The results of calculations in terms of average vertical pressure ($\bar{q}/k_t$) on OD are shown in Fig. 4 as functions of $\gamma H/k_t$ (dotted lines) for the friction angle of the matrix material of 40° and different slope inclination angles. Solutions with a continuous stress field can be obtained only in a limited range of $\gamma H/k_t$, as indicated in Fig. 4 by the extent of the broken lines. These solutions are, therefore, not applicable to slopes with no load ($\bar{q}/k_t = 0$) or to lightly loaded slopes. This is a significant restriction of the continuum approach as applied to reinforced slopes.

STRUCTURAL APPROACH

Granular soil and the reinforcement are now considered as two separate constituents of the structure. The granular matrix is considered to obey the Mohr-Coulomb yield condition and the associative flow rule. The latter leads to zero energy dissipation in the granular matrix during plastic deformation. The upper bound theorem states that *in any kinematically admissible failure mechanism the rate of work done by tractions and body forces is less than or equal to the energy dissipation*

$$\int_v \sigma_{ij}^* \dot{\epsilon}_{ij}^* \, dv \geq \int_S \mathbf{T}_i \mathbf{V}_i \, ds + \int_v \mathbf{X}_i \mathbf{V}_i^* \, dv; \qquad i, j = 1, 2, 3 \tag{16}$$

where $\dot{\varepsilon}_{ij}^*$ = the strain rate in a kinematically admissible velocity field; $\dot{\varepsilon}_{ij}^* = -(\mathbf{V}_{i,j}^* + \mathbf{V}_{j,i}^*)/2$; velocity $\mathbf{V}_i^* = \mathbf{V}_i$ on boundary S (given boundary condition); σ_{ij}^* = stress tensor associated with $\dot{\varepsilon}_{ij}^*$; $\mathbf{X}_i$ = vector of distributed body forces (e.g., the weight); and S and v = loaded boundary and volume, respectively. It is then possible to find an upper bound to the true limit load through equating the rate of work of external forces to the rate of internal energy dissipation. However, this is possible only if the extent of boundary S is given, and the distribution of velocity on S is uniform. Note that in the slope stability problem, used here to illustrate the application of the method, both the pressure $\bar{q}$ and the length of boundary OD [Fig. 5(a)] are unknown, and only OA is fixed (toe failures are considered).

For the case of a slope as in Fig. 5(a), the theorem allows one to write

$$\int_v k_t \langle \dot{\varepsilon}_t \rangle \, dv \geq \int_{OD} \mathbf{q}_i \mathbf{V}_i \, dS + \int_v \boldsymbol{\gamma}_i \mathbf{V}_i^* \, dv; \qquad i = 1, 2 \tag{17}$$

where k_t = tensile strength of reinforcement per unit cross section of the composite; $\langle \dot{\varepsilon}_t \rangle$ = strain rate in the direction of reinforcement (zero if compression)

$$\langle \dot{\varepsilon}_t \rangle = \begin{cases} |\dot{\varepsilon}_t| \text{ when } \dot{\varepsilon}_t < 0 \\ 0 \text{ when } \dot{\varepsilon}_t \geq 0 \end{cases} \tag{18}$$

$\mathbf{q}_i$ = traction vector on OD; and $\boldsymbol{\gamma}_i$ = unit weight vector. The reinforcement here is assumed to dissipate energy during incipient collapse only in the tensile mode (flexible reinforcement, with no resistance to shear and compression). The term on the left-hand side of (17) can alternatively be written as the sum of dissipation rates in all reinforcement layers. Representing reinforcement through parameter k_t is more characteristic to the continuum approach; it is used here in the structural approach to avoid introducing one additional parameter (spacing and single reinforcement strength instead of k_t). The structural approach is distinguished from the continuum approach in that the fill and reinforcement are regarded as two separate structural components in the analysis, and this is done here, even if the reinforcement is represented by parameter k_t.

Good estimates of limit loads from the kinematics-based approach can be obtained by considering a collapse mechanism where geometrical parameters are variable and are varied in an optimization scheme where the least limit load is sought. Only the tensile failure of the reinforcement is considered here, assuming that the length of reinforcement is large enough to prevent pull-out failure. Slip (pullout or sliding over geotextile reinforcement) can be accommodated in the analysis, however, as dissipative terms on the left-hand side of (17). Calculations of the energy dissipation rate during pullout may require that the stress normal to the reinforcement be assumed (typically specific weight of the fill × reinforcement depth is assumed in limit equilibrium methods). Such an additional assumption relaxes the rigorous character of the kinematical approach, and the results can no longer be proved as upper bounds.

The collapse mechanism considered is shown in Fig. 5(a). It consists of rigid blocks separated by rupture surfaces. Kinematical admissibility requires that all velocity jump vectors be inclined

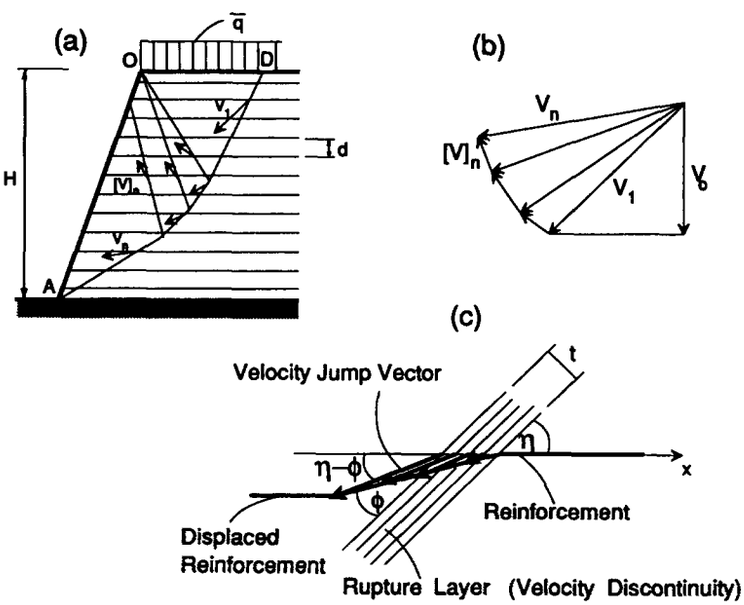

FIG. 5. Structural Approach: (a) Slope Collapse Mechanism; (b) Hodograph; and (c) Deformation of Reinforcement at Rupture Layer

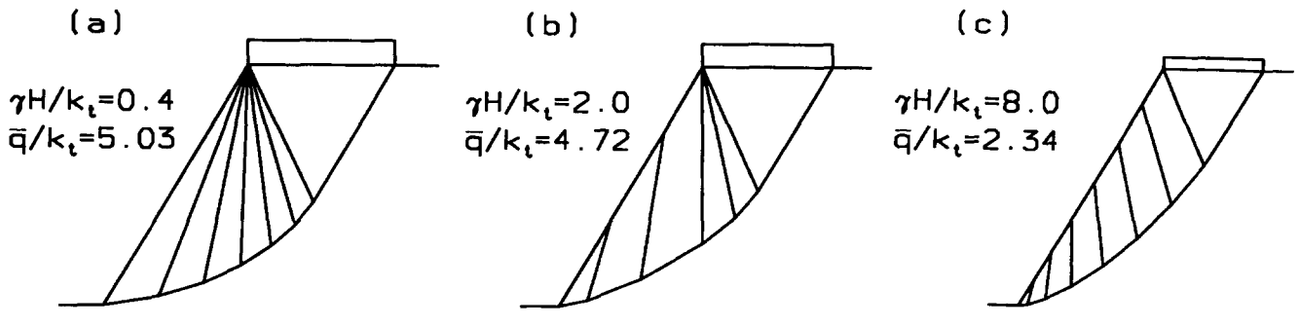

FIG. 6. Examples of Critical Mechanisms (φ = 30°, β = 60°)

at φ to the rupture surfaces. The hodograph is shown in Fig. 5(b). The incipient failure pattern includes only the translation of blocks (no rotation).

In the rigid-block collapse mechanism considered, all energy dissipation in the reinforcement takes place along the velocity discontinuities. The energy dissipation rate per unit area of velocity discontinuity surface is

$$\dot{d} = \int_0^{t/\sin\eta} k_t \dot{\varepsilon}_x \sin\eta \, dx = k_t[V]\cos(\eta - \varphi)\sin\eta \tag{19}$$

Fig. 5(c) explains how (19) was arrived at. The left side of inequality (17) can now be replaced with

$$\dot{D} = \sum_n l k_t[V]\cos(\eta - \varphi)\sin\eta \tag{20}$$

where n = number of straight-line velocity discontinuity segments; l = length of a single discontinuity; $[V]$ = magnitude of the velocity jump across that discontinuity; η = angle of inclination of the reinforcement to the rupture surface (velocity discontinuity); and φ = internal friction angle of the granular matrix. Here, the direction of reinforcement coincides with the x-axis (α = 0).

Examples of specific failure patterns associated with the least value of $\bar{q}$ for 60° slopes characterized by different $\gamma H/k_t$, are presented in Fig. 6 (reinforcement is not shown to preserve the clarity of the failure patterns). The maximum number of blocks used in the analysis was eight. It was found that, for the range of parameters used in the analysis, an increase in the number of blocks beyond eight produced little improvement in the limit load (less than 1%). Results of calculations are presented in Figs. 4 and 7 in a dimensionless manner, with $\bar{q}/k_t$ as functions of $\gamma H/k_t$ for different slope inclinations and different internal friction angles of the matrix material. In each series of calculations (for different β and φ) an optimization scheme was used (with variable geometrical parameters) so that the least $\bar{q}/k_t$ was obtained.

It is surprising at first, that, for each inclination angle, the average $\bar{q}/k_t$ from the structural approach becomes lower than that from the slip-line solution. Although the slip-line solution presented earlier is not a rigorous lower bound, such solutions are usually very good approximations of limit loads and are typically lower than least upper bounds. The stability of slopes, reinforced or not, is an ill-posed problem in that the length of the loaded boundary [OD in Figs. 3(a) and 5(a)] is not given a priori, but is part of the solution. The length of the loaded boundary was unknown in both approaches used. For the same slope and reinforcement, the two techniques produce solutions where the loaded boundary is of a different length. Comparing the average limit pressures from the two solutions is then like comparing bearing capacities (per unit length) of two foundations of different widths. This is the source of the surprising result in Fig. 4, where the slip-line method gives an average limit pressure higher (in some range of parameters) than that from the upper bound approach of limit analysis.

Rotational failure patterns were also tried with the structural approach, and preliminary calculations indicate (as expected) that they predict better (lower) upper bounds to critical heights of slopes that are lightly loaded.

APPLICATION OF CHARTS AND COMPARISON TO OTHER METHODS

It needs to be emphasized that the charts presented in Figs. 4 and 7 are not meant to be a comprehensive design tool; no reinforcement slip is considered here, and only the translational-type failure pattern was considered when developing the charts. The two examples demonstrate the possible application of charts.

In example 1, a slope 6-m high is to be designed. Inclination angle β = 70°, internal friction angle of the fill φ = 35°, unit weight γ = 18 kN/m^3, and the reinforcement to be used has a tensile strength of T = 30 kN/m. The safety factors to be used are as follows: for the soil F_s =

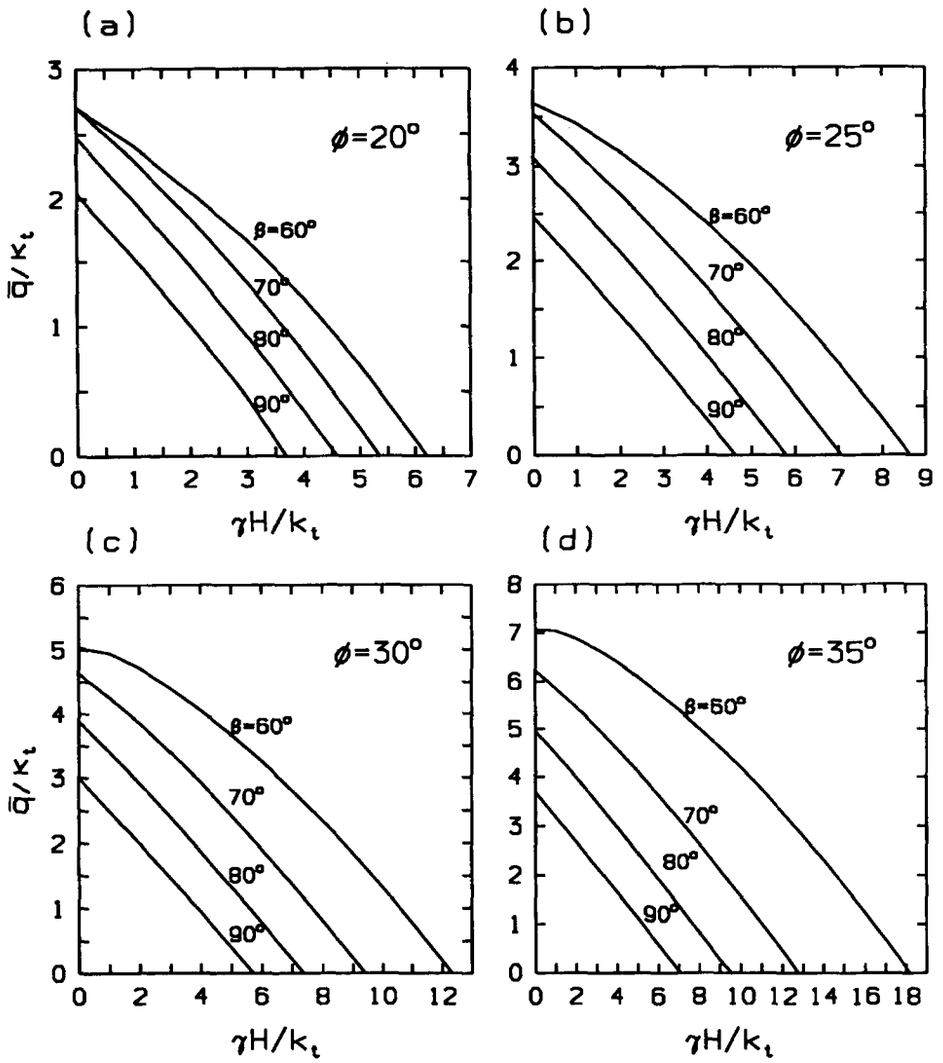

FIG. 7. Average Limit Pressure on Slopes as Function of Slope Characteristic Number $\gamma H/k_t$: (a) φ = 20°; (b) φ = 25°; (c) φ = 30°; and (d) φ = 35°

1.5, and for the reinforcement $F_r = 1.8$. The slope is not loaded at the top surface ($\bar{q}/k_t = 0$). The design value of the internal friction angle of the fill is $\varphi_{ri} = \arctan[(\tan 35°)/F_s] \approx 25°$. From Fig. 7(b), the value of parameter $\gamma H/k_t = 7.1$ (the exact value calculated is 7.063). The required value of the average reinforcement strength in the slope is then $k_t = \gamma H/7.1 = 15.21$ kN/m^2, and, including the safety factor, $k_t = F_r \times 15.21 = 27.38$ kN/m^2. The spacing of the reinforcement, if assumed uniform, is $d = T/k_t = 30/27.38 = 1.096$ m, and we assume $d = 1.0$ m. Alternatively, the number of reinforcing layers can be calculated: $n = k_t H/T = 27.38 \times 6/30 = 5.48 \approx 6$.

In example 2, the data are the same as in example 1, but the slope is loaded with $\bar{q} = 15$ kN/m^2. The procedure of finding the amount of reinforcement is now iterative. From the first example we know that $k_t = 15.21$ kN/m^2 when $\bar{q} = 0$. We take the first guess of k_t as 17 kN/m^2, thus $\gamma H/k_t = 6.35$ and, from Fig. 7(b), $\bar{q}/k_t = 0.42$ and $\bar{q} = 7.14$ kN/m^2. Increasing k_t to 18 kN/m^2 leads to $\gamma H/k_t = 6.0$, $\bar{q}/k_t = 0.62$ and $\bar{q} = 11.16$ kN/m^2, and, for $k_t = 19$ kN/m^2, one obtains $\gamma H/k_t = 5.68$, $\bar{q}/k_t = 0.80$, and $\bar{q} = 15.20$ kN/m^2. The required k_t is then 19 kN/m^2 and, including the safety factor, $k_t = 34.2$ kN/m^2. The number of layers necessary to reinforce the slope is now $n = k_t H/T = 34.2 \times 6/30 = 6.84 \approx 7$.

To indicate whether considerations based on the continuum and structural approaches presented lead to reasonable predictions, the results are compared to three experiments. A wall described by Bathurst and Benjamin (1990), 3-m tall ($H = 3$ m), reinforced with four layers of geogrid, was loaded to failure at 80 kPa. The average bulk density of the fill was estimated as $\rho = 1.8$ Mg/m^3, and the internal friction angle of the fill (from a large-scale shear box) was determined as changing from 56° at 10 kPa to 43° at 120 kPa (secant). For other properties see the paper by Bathurst and Benjamin (1990). Calculations were performed for the two external magnitudes of φ. The failure loads calculated from the continuum approach are 62 kPa and 145

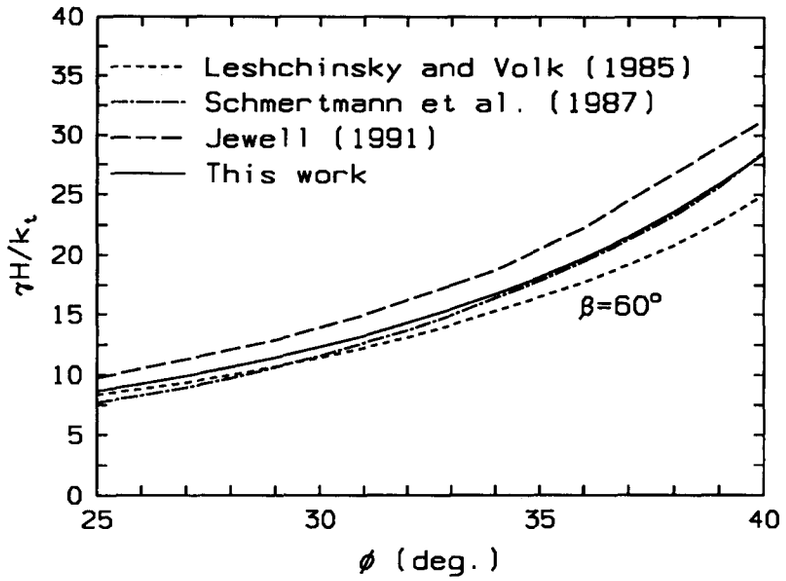

FIG. 8. Comparison of Critical Slope Heights Predicted by Different Methods

kPa, and from the structural approach 57 kPa and 144 kPa, respectively. Both methods predict the exact failure load $\bar{q} = 80$ kPa when the internal friction is taken between 47° and 48°. Calculations for a pressure-dependent friction of the fill were not performed, but when the secant friction angle is assumed to be changing linearly between 10 kPa and 120 kPa, and the "representative" friction angle is assumed to be that at pressure equal to $\bar{q} + \gamma H/2$, the failure load calculated from the structural approach becomes 70 kPa.

The other two walls for which the proposed methods are used here are those described by Wu (1992). Reinforced walls of 3-m height, one with granular fill, and one with cohesive fill were loaded until failure. The soil and geosynthetic parameters can be found in Wu (1992). For the granular fill wall, the failure load was 200 kPa (29 psi), whereas the estimate by the continuum approach proposed here was 123 kPa and 122 kPa using the structural approach. The internal friction angle used was determined through triaxial tests as 39°. Under plane strain conditions this angle can be expected to be larger, and for instance, for 43° (an arbitrary increase of 10%) the failure load predictions are 153 kPa and 152 kPa, respectively. For the cohesive soil wall the tested failure load was 227 kPa (33 psi), and the predictions with the soil parameters from the consolidated undrained tests are 216 kPa and 215 kPa, respectively.

These comparisons indicate that the techniques suggested for including the reinforcement in the stability analyses give very reasonable predictions, and they may prove to be useful tools in design with geosynthetics.

The results from the proposed structural approach are compared to those by Leshchinsky and Volk (1985), Schmertmann et al. (1987), and Jewell (1990). Fig. 8 shows the respective results in terms of dimensionless critical heights of slopes $\gamma H/k_t$ ($\bar{q}/k_t = 0$) as a function of the internal friction angle of the fill (cohesionless). The parameter k_t is introduced in this paper to represent reinforcement [(3)], and the solutions of other authors were recalculated accordingly. The structural approach solution is a rigorous upper bound to critical heights where forces in the entire reinforcement are fully mobilized, while in solutions by Leshchinsky and Volk (1985), and Schmertmann et al. (1987), the forces in the reinforcement are not assumed fully mobilized in all layers. It is surprising that the revised method by Jewell (1990), which is based on the log-spiral failure surface, leads to a higher estimate of the critical height. The writers' experience for unreinforced slopes indicates that rotational failure mechanisms yield the least upper bounds to critical heights of load-free slopes. The solution according to Jewell (1990) overestimates the nondimensional critical height, with respect to the structural approach presented here, by 12–15% for the 60° slope. It is fair to conclude, however, that all four methods produce reasonably close results.

FINAL REMARKS

Two methods were described for analysis of reinforced soil structures: a continuum approach based on introducing the macroscopic failure criterion for the homogenized reinforced soil composite, and the structural approach, where the fill and the reinforcement are considered as two separate structural constituents. It was found that the continuum approach with the slip-line solution methods has some disadvantages when compared to the structural approach. The

slip-line method, for instance, does not allow one to obtain solutions for arbitrarily loaded slopes; for instance, it cannot be used to calculate the critical height of the slope with a zero load. Including the nonuniform distribution of reinforcement in the continuum approach would contribute to a significant increase in the complexity of the solution (solving for the stress field in nonhomogeneous and anisotropic soil). In the structural approach, the nonuniform distribution can be dealt with in a simpler manner.

It is concluded that the structural approach to the stability analysis of traditionally reinforced soil (unidirectionally placed bars, strips, geosynthetic sheets, or geogrids) is more convenient and more useful than the continuum approach. The continuum approach, however, is likely to find a wider application in the analysis of less conventional reinforcements, such as continuous filament and fiber-reinforced soils.

Simple limit-equilibrium considerations, such as two-block failure mechanisms for slopes, have been successful in design, but not necessarily because they are good models of the true failure processes. They often include assumptions not consistent with the limit-equilibrium concept (for instance, reinforcement forces that are not at all at their limit). The shortcomings of the mechanics considerations are then compensated for by the "hidden" safety factors following from such assumptions, and the final outcome seems to be satisfactory for practical use. The writers' intent was to point out that a more rigorous approach can be applied with little extra effort to obtain results that have a clear theoretical interpretation. The writers believe that improvement to design methods should come through more rigorous mechanics considerations before factors including technology of construction, durability, and so on, can be introduced with a reasonable level of confidence. Comparison of the calculations to experimental tests with reinforced slopes indicates that the structural approach is a very reasonable method for analysis of reinforced soil structures.

The structural approach suggested here as a design tool is obtained by equating the work rate of external forces to the rate of internal energy dissipation in a kinematically admissible collapse mechanism. The forces associated with such mechanism, although not calculated here, can be proved to satisfy the force equilibrium equations (Mróz and Drescher 1969; Collins 1974; Michalowski 1989; Salençon 1990; Drescher and Detournay 1993). This is emphasized, since the limit equilibrium method is very widely accepted in geotechnical engineering, whereas the upper-bound approach is often discounted as an "unsafe" method.

The kinematical technique of limit analysis often draws criticism because of the use of the normality rule, which leads to overestimating the true dilatancy of the soil. It can be demonstrated that the traditional limit equilibrium method leads to the same rule, even if not used explicitly in the solution technique. The structural approach based on kinematic limit analysis can be modified easily to include incompressibility or less dilatancy than that resulting from the associated flow rule (Drescher and Detournay 1993). Such modification can also be introduced into the limit equilibrium method but not without first giving consideration to the kinematics of the plastic flow of soils.

ACKNOWLEDGMENT

The material presented in this paper is based on work supported by the National Science Foundation under Grant No. MSS-9301494. This support is gratefully acknowledged.

APPENDIX I. REFERENCES

Anthoine, A. (1989). "Mixed modeling of reinforced soils within the framework of the yield design theory." *Comp. and Geotechnics*, 7(1&2), 67–82.

Bathurst, R. J., and Benjamin, D. J. (1990). "Failure of a geogrid-reinforced soil wall." *Transp. Res. Rec. 1288*, Transportation Research Board, Washington, D.C., 109–116.

Booker, J. R., and Davis, E. H. (1972). "A general treatment of plastic anisotropy under conditions of plane strain." *J. Mech. Phys. Solids*, 20(4), 239–250.

de Buhan, P., Mangiavacchi, R., Nova, R., Pellegrini, G., and Salençon, J. (1989). "Yield design of reinforced earth walls by homogenization method." *Géotechnique*, London, England, 39(2), 189–201.

de Buhan, P., and Siad, L. (1989). "Influence of a soil-strip interface failure condition on the yield-strength of reinforced earth." *Comp. and Geotechnics*, 7(1&2), 3–18.

De Buhan, P., and Taliercio, A. (1991). "A homogenization approach to the yield strength of composite materials." *Eur. J. Mech., Ser. A/Solids*, Montrouge, France, 10(2), 129–154.

Collins, I. F. (1974). "A note on the interpretation of Coulomb's analysis of the thrust on a rough retaining wall in terms of the limit theorems of plasticity theory." *Géotechnique*, London, England, 24, 106–108.

Drescher, A., and Detournay, E. (1993). "Limit load in translational failure mechanisms for associative and non-associative materials." *Géotechnique*, London, England, 43, 443–456.

Jewell, R. A. (1990). "Revised design charts for steep reinforced slopes. *Reinforced embankmanets, theory and practice*, Thomas Telford, London, England, 1–30.

Leshchinsky, D., and Volk, J. C. (1985). "Stability charts for geotextile-reinforced walls." *Transp. Res. Rec. 1131*, Transportation Research Board, Washington, D.C., 5–16.

McLaughlin, P. V., and Batterman, S. C. (1970). "Limit behavior of fibrous materials." *Int. J. Solids Struct.*, 6(10), 1357–1376.

Michalowski, R. L. (1989). "Three-dimensional analysis of locally loaded slopes." *Géotechnique*, London, England, 39(1), 27–38.

Michalowski, R. L. (1992). "Stability of embankments over weak soils of limited thickness." *Grouting, soil improvement and geosynthetics*, Vol. 2, ASCE, New York, N.Y., 1142–1152.
Michalowski, R. L., and Zhao, A. (1993). "Failure criteria for homogenized reinforced soils and application in limit analysis of slopes. " *Proc., Geosynthetics '93*, Vol. 1, Industrial Fabrics Association Int., St. Paul, Minn., 443–453.
Michalowski, R. L., and Zhao, A. (1994). "Limit loads on fiber-reinforced earth structures." *Proc., XIII ICSMFE*, Balkema, Rotterdam, Vol. 2, 809–812.
Mróz, Z., and Drescher, A. (1969). "Limit plasticity approach to some caes of flow of bulk solids." *J. Engrg. for Industry, Trans. ASME*, 91(2), 357–364.
Romstad, K. M., Hermann, L. R., and Shen, C. K. (1976). "Integrated study of reinforced earth—I: theoretical formulation." *J. Geotech. Engrg. Div.*, ASCE, 102(5), 457–471.
Salençon, J. (1990). "An introduction to the yield design theory and its applications to soil mechanics." *Eur. J. Mech., Ser. A/Solids*, 9(5), 477–500.
Sawicki, A. (1983). "Plastic limit behavior of reinforced earth." *J. Geotch. Engrg.*, ASCE, 109(7), 1000–1005.
Sawicki, A., and Leśniewska, D. (1989). "Limit analysis of cohesive slopes reinforced with geotextiles." *Comp. and Geotechnics*, 71(1&2), 53–66.
Schmertmann, G. R., Chourery-Curtis, V. E., Johnson, R. D., and Bonaparte, R. (1987). "Design charts for geogrid-reinforced soil slopes." *Proc., Geosynthetics '87*, Vol. 1, Industrial Fabrics Association Int., St. Paul, Minn., 108–120.
Sokolovskii, V. V. (1965). *Statics of granular media*. Pergamon Press, New York, N.Y.
Wu, J. T. H. (1992). "Predicting performance of the Denver walls: general report." *Proc., Int. Symp. Geosynthetic-Reinforced Soil Retaining Walls*, J. T. H. Wu, ed., A. A. Balkema, Rotterdam, The Netherlands, 3–20.

APPENDIX II. NOTATION

The following symbols are used in this paper:

d = spacing of reinforcement layers;
H = slope height;
k_t = tensile strength of reinforcement per unit area of composite;
p, q = stress parameters; $p = (\bar{\sigma}_x + \bar{\sigma}_y)/2$, $q = (\bar{\sigma}_x - \bar{\sigma}_y)/2$;
$\bar{q}$ = average vertical limit pressure on slope;
R = stress invariant;
T = tensile strength of reinforcement per unit length;
$\mathbf{T}_i$ = vector of traction;
t = rupture layer thickness;
$[V]$ = magnitude of velocity jump vector;
$\mathbf{V}_i$ = velocity vector;
α = inclination angle of reinforcement to x-axis;
β = slope inclination angle;
γ = unit weight of soil;
$\dot{\boldsymbol{\varepsilon}}_{ij}$ = strain rate tensor;
η = inclination angle of reinforcement to rupture surface;
ξ = coefficient of mobilization of reinforcement strength;
$\boldsymbol{\sigma}_{ij}^{(\cdot)}$ = stress state in composite constituents;
$\bar{\boldsymbol{\sigma}}_{ij}$ = macroscopic stress tensor;
$\bar{\tau}_{xy}$ = macroscopic shear stress in composite;
φ = internal friction angle of fill; and
ψ = inclination angle of major principal macroscopic stress to x-axis.